Structural and insulator-to-metal phase transition at 50 GPa in $GdMnO_3$

J. Oliveira,[1] J. Agostinho Moreira,[1,*] A. Almeida,[1] V. H. Rodrigues,[2] M. M. R. Costa,[2] P. B. Tavares,[3] P. Bouvier,[4,5] M. Guennou,[4] and J. Kreisel[4]

[1]*IFIMUP and IN-Institute of Nanoscience and Nanotechnology, Departamento de Física e Astronomia, Faculdade de Ciências, Universidade do Porto, Rua do Campo Alegre, 687, 4169-007 Porto, Portugal*

[2]*CEMDRX, Departamento de Física, Faculdade de Ciências e Tecnologia, Universidade de Coimbra, 3004-516 Coimbra, Portugal*

[3]*Centro de Química, Universidade de Trás-os-Montes e Alto Douro, Apartado 1013, 5001-801, Vila Real, Portugal*

[4]*Laboratoire des Matériaux et du Génie Physique, CNRS, Grenoble Institute of Technology, MINATEC, 3 Parvis Louis Néel, 38016 Grenoble, France*

[5]*European Synchrotron Radiation Facility (ESRF), 6 Rue Jules Horowitz, F-38043 Grenoble Cedex, France*

(Received 25 October 2011; published 23 February 2012)

We present a study of the effect of very high pressure on the orthorhombic perovskite $GdMnO_3$ by Raman spectroscopy and synchrotron x-ray diffraction up to 53 GPa. The experimental results yield a structural and insulator-to-metal phase transition close to 50 GPa, from an orthorhombic to a metrically cubic structure. The phase transition is of first order with a pressure hysteresis of about 6 GPa. The observed behavior under very high pressure might well be a general feature in rare-earth manganites.

DOI: 10.1103/PhysRevB.85.052101 PACS number(s): 71.30.+h, 62.50.−p, 71.27.+a, 75.47.Lx

Rare-earth manganites have attracted continuous attention for their complex correlations among lattice, electric, and magnetic degrees of freedom. More recently, magnetoelectric and multiferroic properties of manganites have attracted a particular interest.[1] Most manganites crystallize at ambient conditions in a *Pnma* structure, which presents distortions away from the ideal cubic perovskite structure through cooperative Jahn-Teller distortion and tilt of the MnO_6 octahedra. Such manganites have been extensively studied as a function of temperature, magnetic field, strain (in thin films), or chemical composition. High pressure is another parameter allowing tuning of different degrees of freedom in manganites, but this remains little explored to date. A notable exception is the study of the crystal structure, Jahn-Teller distortion, orbital order, and pressure-induced insulator-metallic phase transition in $LaMnO_3$, although the driving mechanism still remains controversial.[2–8] According to the pioneer work by Loa *et al.*,[2] the Jahn-Teller effect and the concomitant orbital ordering are suppressed above 18 GPa. The system retains insulator behavior up to 32 GPa, undergoing a bandwidth-driven insulator-metal phase transition. Other authors have reported the persistence of the Jahn-Teller distortion over the entire stability range of the insulating phase of $LaMnO_3$, suggesting a nonclassical Mott insulator.[3,6] No other orthorhombic manganite has attracted such an attention, although we note the pressure investigation of structural properties of the magnetoelectric manganites $TbMnO_3$ and $DyMnO_3$ or $BiMnO_3$, or more complex solid solutions.[9–11] To the best of our knowledge, manganites have not yet been investigated in the very-high-pressure regime around 50 GPa, despite promising studies on similar orthoferrites or $BiFeO_3$, which have revealed intriguing insulator-to-metal or structural transitions in a similar pressure range.[12–15]

The aim of this work is to explore the effect of very high pressure on rare-earth manganites. We chose $GdMnO_3$, which is currently attracting considerable attention as a frustrated magnetic system for which a ferroelectric order can be induced by application of a modest magnetic field.[16–18] Its phase diagram has been extensively studied as a function of external parameters: temperature, doping, and high magnetic fields.[16,18,19] Pressure has only been explored up to 1 GPa through a pressure-dependent study of the dielectric constant at low temperatures.[20] Here, we report a pressure-dependent investigation of the lattice dynamics and crystal structure of $GdMnO_3$ at room temperature up to 53 GPa, through Raman spectroscopy and x-ray powder diffraction.

High-quality ceramic $GdMnO_3$ samples were prepared using the sol-gel urea combustion method (see Ref. 21), and their chemical, morphological, and structural characteristics were checked by x-ray, scanning electron microscopy, Energy-dispersive x-ray spectroscopy, and x-ray photoemision spectroscopy. A powder sample was loaded in a Diamond Anvil Cell (DAC) with diamond tips of diameter 300 μm and with helium as a pressure-transmitting medium. The Raman spectra were recorded on a LabRam spectrometer using a He-Ne laser at 633 nm. The laser power was kept below 5 mW on the DAC to avoid sample heating. High-pressure angle dispersive synchrotron x-ray diffraction (XRD) experiments were performed at the European Synchrotron Radiation Facility (ESRF) on the ID27 high-pressure beam line. XRD patterns were collected on a Mar charge coupled device detector with a focused monochromatic beam at $\lambda = 0.3738$ Å. The powder diffraction data were analyzed by full Rietveld refinements using the FullProf software.[22] Rare-earth manganites, which crystallize in the *Pnma* structure, present 24 Raman active modes.[23] In our unpolarized Raman setup, all Raman-active modes can be observed. The Raman spectra of $GdMnO_3$ have been studied by several authors both at low temperatures and under high magnetic field.[23–25]

Lavèrdiere *et al.*[24] proposed that the intense Raman bands in rare-earth manganites are of A_g and B_{2g} symmetry, and this was confirmed by a study of Y-doped $EuMnO_3$.[26] Iliev *et al.*[23] presented the mode assignment of various rare-earth manganites together with the atomic motions involved in each mode.

Figure 1(a) presents selected Raman spectra of $GdMnO_3$ for increasing pressures up to 53 GPa, recorded at room

 ©2012 American Physical Society

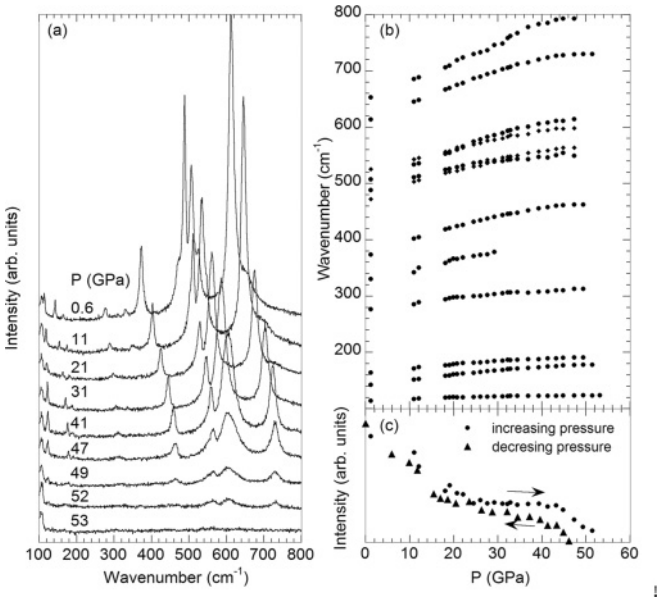

FIG. 1. (a) Evolution of the Raman spectra and (b) Raman shifts for all bands with increasing pressure. (c) Intensity of the Raman mode at initially 610 cm^{-1} upon increasing and decreasing pressure.

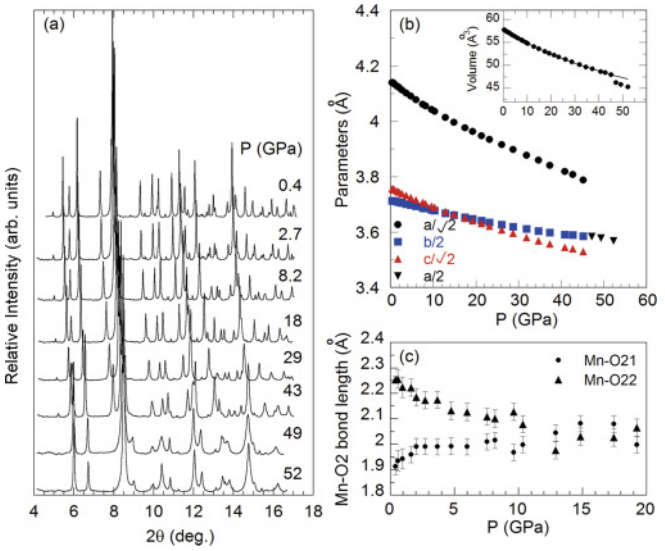

FIG. 2. (Color online) Evolution of the (a) XRD pattern, (b) pseudocubic parameters and volume, and (c) Mn-O2 bond lengths under pressure. The solid line in the insert of Fig. 2(b) was calculated from the best fit of the third-order Birch-Murnaghan equation to the volume data.

temperature. The spectrum at ambient conditions is consistent with literature data (see Refs. 23,24) and is characterized by 12 bands, with prominent features at 610 cm^{-1} (B_{2g} Jahn-Teller symmetric stretching mode), 502 cm^{-1} (A_g bending mode), 487 cm^{-1} (A_g Jahn-Teller asymmetric stretching mode), 373 cm^{-1} (A_g mode, tilt of the MnO_6 octahedra around [101]), and 275 cm^{-1} (A_g mode, tilt of the MnO_6 octahedra around [010]). The two shoulders at 473 cm^{-1} and at 522 cm^{-1} correspond to bending of MnO_6 octahedra and scissor-like oxygen rotations modes of symmetry B_{2g}, respectively.

With increasing pressure toward 45 GPa, all Raman bands shift to higher wave numbers, as expected for pressure-induced bond shortening. Within this pressure range, the changes in the spectral signature can be entirely explained by increasing line width, band overlap, and a decreasing intensity, suggesting that $GdMnO_3$ undergoes no phase transition up to 45 GPa.

TABLE I. Raman line wave number, symmetry, and pressure-dependence slope of $GdMnO_3$ measured at room temperature conditions.

ω_o (cm^{-1})	Symmetry	Slope (cm^{-1}/GPa)
114		0.03(3)
141	B2g or B3g	0.96(3)
163	B2g or B3g	0.78(4)
275	Ag	1.06(5)
326	B2g	1.9(1)
373	Ag	2.47(8)
473	B2g	2.4(1)
487	Ag	2.02(4)
502	Ag	2.82(8)
522	B2g	1.88(6)
610	B2g	3.10(3)
648		3.31(9)

This observation is supported by the pressure evolution of the Raman shifts for the different bands, which show different slopes but no anomaly (Fig. 1). In the range from 0.1 to 20 GPa, the wave number of each band can be approximated by a linear function of pressure, the slopes for which are presented in Table I. We note that two pairs of modes at 473/487 cm^{-1} and 502/522 cm^{-1} cross upon increasing pressure, which is allowed by their different symmetries. Between 45 GPa and about 49 GPa, the wave number of all Raman bands keeps constant, while the bands broaden and decrease in intensity.

The most notable result of Fig. 1(a) is the complete extinction of the Raman signature at 53 GPa. As an example, Fig. 1(c) shows the pressure dependence of the intensity of the band associated with the in-phase O2 stretching mode at initially 610 cm^{-1}, which decreases gradually and eventually vanishes above 51 GPa. This suppression is a clear sign for a phase transition at very high pressure. The transition is reversible, as illustrated through the recovery with decreasing pressure of the intensity of the in-phase O2 stretching mode as shown in Fig. 1(c). The Raman spectrum is only recovered after decreasing pressure just below 47 GPa, indicating an important pressure hysteresis of 6 GPa, which strongly suggests a first-order phase transition.

While this signature provides conclusive evidence for a phase transition, the evolution of the Raman spectra alone does not allow its nature to be elucidated. Two main scenarios can be envisaged: (i) Under high-pressure, $GdMnO_3$ shows a phase transition from the *Pnma* structure to the ideal perovskite *Pm-3m* structure. In this scenario, the loss of the Raman spectra is explained by the fact that Raman scattering is forbidden by symmetry in the ideal perovskite structure. The choice of this structure is unique, since Raman scattering is not forbidden for any other perovskite structure. (ii) Under high pressure, $GdMnO_3$ undergoes a transition from an insulator to a metal (possibly accompanied by a change in the magnetic order),

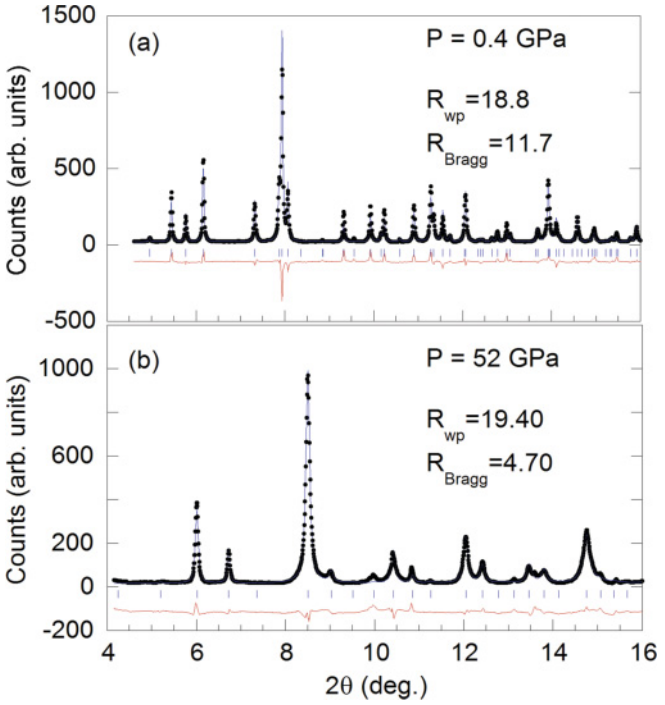

FIG. 3. (Color online) Experimental, calculated, and difference in XRD patterns (a) at 0.4 GPa in the *Pnma* phase and (b) at 52 GPa in the $P2_13$ phase.

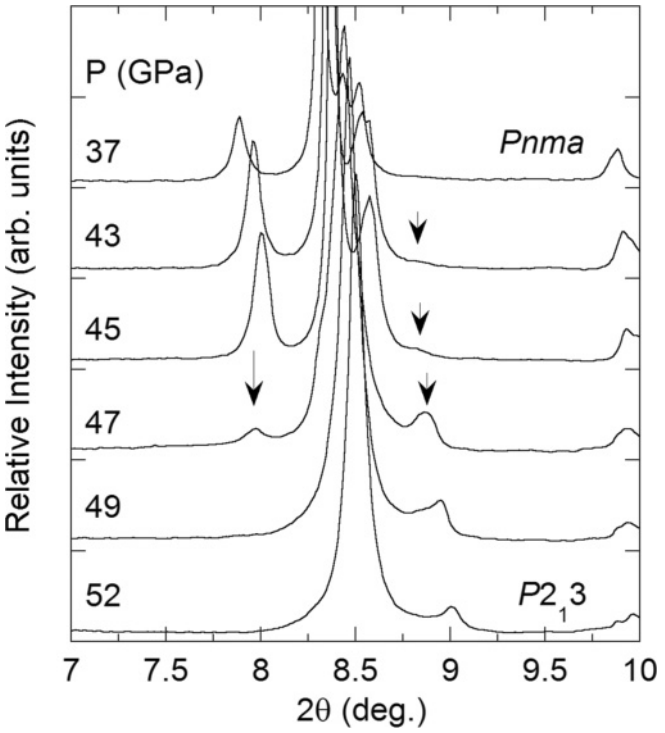

FIG. 4. XRD patterns in the 7° to 10° 2θ range ($\lambda = 0.3738$ Å), from 37 and 52 GPa.

similar to what has been observed in a similar pressure range for orthoferrites or $BiFeO_3$.[12–14] Here, the loss of the Raman spectrum is explained by the free-electron screening in the metallic phase, enhancing the reflectivity of the sample. This fact in turn inhibits the observation of a signal, which is already weak for the black samples in the insulator phase. A combination of (i) and (ii), i.e., a transition toward a metallic cubic *Pm-3m* phase, is of course also possible.

In order to elucidate which of the models can best explain the observed transition, we have undertaken a pressure-dependent synchrotron x-ray diffraction experiment up to 52 GPa. Figure 2(a) shows representative powder x-ray patterns collected at room temperature for different pressures. An inspection of the diffraction data shows that $GdMnO_3$ maintains the characteristic diffraction pattern of a *Pnma* structure up to 45 GPa. Above this pressure, the diffraction pattern changes significantly toward a pattern with fewer Bragg reflections, suggesting an increase in symmetry. Most Bragg reflections of the new high-pressure phase are broader than in the low-pressure phase.

In order to discuss the structural evolution in the low-pressure phase, we have carried out full Rietveld refinements of all diffraction patterns up to a pressure of 45 GPa by assuming a *Pnma* space group, which allows a reliable fit of the whole diffraction pattern. Figure 3(a) illustrates the quality of a representative refinement at a pressure of 0.4 GPa. The analysis of the diffraction pattern obtained between 45 and 49 GPa is less straightforward, due to a phase coexistence with overlapping and broadening of reflections. In order to document the coexistence of phases in the 45 to 49 GPa pressure range, we have plotted in Fig. 4 the XRD patterns in the 7° to 10° 2θ range. The phase coexistence in the pressure

TABLE II. Wyckoff positions and atomic coordinates obtained from the Rietveld refinement of the x-ray diffractogram recorded at 0.4 GPa and 52 GPa.

Pressure (GPa)	Atom	Wyckoff position	x	y	z
0.4	Gd	4c	0.5812(4)	0.250	0.5203(6)
	Mn	4c	0.00	0.00	0.500
	O1	4b	−0.033(4)	0.250	0.394(4)
	O2	8d	0.164(4)	0.548(2)	0.196(3)
52	Gd1	4a	−0.021(1)	−0.021(1)	−0.021(1)
	Gd2	4a	0.516(1)	0.516(1)	0.516(1)
	Mn1	4a	0.277(1)	0.277(1)	0.277(1)
	Mn2	4a	0.739(3)	0.739(3)	0.739(3)
	O1	12b	0.340(6)	0.310(8)	0.014(7)
	O2	12b	0.297(6)	0.235(8)	0.469(5)

range referred to above is revealed by the simultaneous emergence of the (200) peak at $2\theta = 8^\circ$ of the *Pnma* phase and the (221) peak at $2\theta = 9^\circ$ of the $P2_13$ phase, indicating also the first nature of the phase transition. Moreover, this phase coexistence is compatible with the wave number saturation observed from the Raman lines in the same pressure range.

By investigating the high-pressure XRD pattern through profile matching, a cubic metric appears to be a good candidate. However, no cubic centered structure, including the Raman-inactive *Pm-3m* structure of the ideal cubic perovskite, can explain the pattern, as we observe a number of superstructure reflections representative of a primitive structure with doubled parameters.

The best profile matching is obtained by assuming $a_{\text{cubic}} = b_{Pnma}$, with a large primitive cell with $V_{\text{cubic}} = 2V_{Pnma}$ and $Z = 8$. Based on this metric, full refinements were tested for all primitive cubic space groups to identify the most appropriate model. The best fit to the experimental data was achieved for space group $P2_13$ (see profile and reliability factors in Fig. 3). Table II presents the Wyckoff positions and the atomic coordinates resulting from the Rietveld refinement at 0.4 GPa and at 52 GPa. Let us note that: (i) this cubic cell and this space group are rather unusual for simple perovskites; and (ii) a factor group analysis of $GdMnO_3$ in the $P2_13$ space group predicts 49 optical modes at the Γ-point of the Brillouin zone, with $\Gamma_{\text{optical}} = 10A + 10E + 29F$. Because the A and E and F modes are Raman-active, the suppression of the Raman spectrum cannot be explained by a structural phase transition, and it more likely results from an insulator-metallic phase transition.

The pressure dependence of pseudocubic lattice parameters $a/\sqrt{2}$, $b/2$, $c/\sqrt{2}$, and volume $V/4$ of the unit cell are shown in Fig. 2(b). Within the orthorhombic phase, the compression is anisotropic with the soft direction along the *a*-axis. We note that the order of the *b* and *c* lattice parameters is inverse with increasing pressure, consistent with the continuous evolution from a Jahn-Teller distorted structure at low pressure to a $GdFeO_3$-type tilted perovskite at high pressure. The pressure dependence of the unit cell volume is adequately described by a third-order Birch-Murnaghan equation[27] up to 45 GPa, yielding $B_o = (175 \pm 2)$ GPa, $B_o' = 3.01 \pm 0.06$, and $V_0 = 230.92$ Å^3 for the bulk modulus, its pressure derivative, and volume at zero pressure, respectively (see solid line in Fig. 2). The 3.6% volume drop observed at the transition for the reduced $Z = 1$ pseudocubic cell is again a signature of a first-order transition.

We now discuss the evolution with pressure of Mn-O bond lengths, deduced from the atomic positions obtained from Rietveld refinement of the x-ray data. The analysis is restricted to data obtained up to 20 GPa. At higher pressures, the broadening of Bragg reflections limits the reliability of the structural data obtained from full Rietveld analysis, in particular, the positions of the light oxygen atoms. Fig. 2(c) shows that the two initially different Mn-O2 distances approach each other with increasing pressure up to 12 GPa. This observation shows that the cooperative Jahn-Teller distortion is reduced with increasing pressure. We cannot argue for a definite suppression of the Jahn-Teller distortion, as the experimental resolution is not high enough. However, our results indicate that the Jahn-Teller distortion is indeed reduced under pressure. It is worth stressing that we observe also at 12 GPa the crossing of the *b* and *c* cell parameters.

In summary, a pressure-dependent study of $GdMnO_3$ using Raman spectroscopy and synchrotron XRD up to 53 GPa yields a phase transition around 50 GPa from an orthorhombic to a cubic structure. Its first-order nature is evidenced by phase coexistence, volume change at the transition, and pressure hysteresis. Raman and XRD allow the phase transition to be identified as being both a structural and an insulator-metallic phase transition. Refinement of pressure data in the *Pnma* structure suggests a decrease of the Jahn-Teller distortion. It is worthwhile to note that the transition at 50 GPa occurs in the very-high-pressure regime, similar to what has been observed in rare-earth orthoferrites or $BiFeO_3$.[12–15] This behavior might well be a general feature in rare-earth manganites under very high pressure.

This work was supported by Fundação para a Ciência e Tecnologia, through Projects PTDC/CTM/67575/2006 and PEst-C/FIS/UI0036/2011. We would like to thank V. Komshenko for helpful discussions. We are grateful to the ESRF staff, especially to G. Garbarino for experiments, and M. Mezouar for allocation of in-house beam time.

*Corresponding author: jamoreir@fc.up.pt

[1] M. Fiebig, J. Phys. D **38**, R123 (2005).
[2] I. Loa, P. Adler, A. Grzechnik, K. Syassen, U. Schwarz, M. Hanfland, G. K. Rozenberg, P. Gorodetsky, and M. P. Pasternak, Phys. Rev. Lett. **82**, 125501 (2001).
[3] M. Baldini, V. V. Struzhkin, A. F. Goncharov, P. Postorino, and W. L. Mao, Phys. Rev. Lett. **106**, 066402 (2011).
[4] M. Baldini, D. Di Castro, M. Cestelli-Guidi, J. Garcia, and P. Postorino, Phys. Rev. B **80**, 045123 (2009).
[5] J. D. Fuhr, M. Avignon, and B. Alascio, Phys. Rev. Lett. **100**, 216402 (2008).
[6] A. Y. Ramos, H. C. N. Tolentino, N. M. Souza, J. P. Itie, L. Morales, and A. Caneiro, Phys. Rev. B **75**, 052103 (2007).
[7] A. Yamasaki, M. Feldbacher, Y. F. Yang, O. K. Andersen, and K. Held, Phys. Rev. Lett. **96**, 166401 (2006).
[8] G. Trimarchi and N. Binggeli, Phys. Rev. B **71**, 035101 (2005).
[9] J. M. Chen, T. L. Chou, J. M. Lee, S. A. Chen, T. S. Chan, T. H. Chen, K. T. Lu, W. T. Chuang, H. S. Sheu, S. W. Chen, C. M. Lin, N. Hiraoka, H. Ishii, K. D. Tsuei, and T. J. Yang, Phys. Rev. B **79**, 165110 (2009).
[10] J. M. Chen, J. M. Lee, T. L. Chou, S. A. Chen, S. W. Huang, H. T. Jeng, K. T. Lu, T. H. Chen, Y. C. Liang, S. W. Chen, W. T. Chuang, H. S. Sheu, N. Hiraoka, H. Ishii, K. D. Tsuei, E. Huang, C. M. Lin, and T. J. Yang, J. Chem. Phys. **133**, 154510 (2010).
[11] A. A. Belik, H. Yusa, N. Hirao, Y. Ohishi, and E. Takayama-Muromachi, Inorg. Chem. **48**, 1000 (2009).

[12]G. Catalan and J. F. Scott, Adv. Mater. **21**, 1 (2009).
[13]A. G. Gavriliuk, V. V. Struzhkin, I. S. Lyubutin, S. G. Ovchinnikov, M. Y. Hu, and P. Chow, Phys. Rev. B **77**, 155112 (2008).
[14]O. E. Gonzalez-Vazquez and J. Íñiguez, Phys. Rev. B **79**, 064102 (2009).
[15]M. Guennou, P. Bouvier, G. S. Chen, B. Dkhil, R. Haumont, G. Garbarino, and J. Kreisel, Phys. Rev. B **84**, 174107 (2011).
[16]T. Kimura, G. Lawes, T. Goto, Y. Tokura, and A. P. Ramirez, Phys. Rev. B **71**, 224425 (2005).
[17]R. Feyerherm, E. Dudzik, A. U. B. Wolter, S. Valencia, O. Prokhnenko, A. Maljuk, S. Landsgesell, N. Aliouane, L. Bouchenoire, S. Brown, and D. N. Argyriou, Phys. Rev. B **79**, 134426 (2009).
[18]T. Arima, T. Goto, Y. Yamasaki, S. Miyasaka, K. Ishii, M. Tsubota, T. Inami, Y. Murakami, and Y. Tokura, Phys. Rev. B **72**, 100102(R) (2005).
[19]J. Baier, D. Meier, K. Berggold, J. Hemberger, A. Balbashov, J. A. Mydosh, and T. Lorenz, Phys. Rev. B **73**, 100402(R) (2006).
[20]K. Noda, S. Nakamura, J. Nagayama, and H. Kuwahara, J. Appl. Phys. **97**, 10C103 (2005).
[21]J. Agostinho Moreira, A. Almeida, W. S. Ferreira, M. R. Chaves, J. B. Oliveira, J. M. Machado da Silva, M. A. Sá, S. M. F. Vilela, and P. B. Tavares, J. Electroceram. **25**, 203 (2010).
[22]J. Rodriguez-Carvajal, Physica B **192**, 55 (1993).
[23]M. N. Iliev, M. V. Abrashev, J. Laverdière, S. Jandl, M. M. Gospodinov, Y.-Q. Wang, and Y.-Y. Sun, Phys. Rev. B **73**, 064302 (2006).
[24]J. Laverdière, S. Jandl, A. A. Mukhin, V. Yu. Ivanov, V. G. Ivanov, and M. N. Iliev, Phys. Rev. B **73**, 214301 (2006).
[25]J. Agostinho Moreira, A. Almeida, J. Oliveira, M. R. Chaves, J. Kreisel, F. Carpinteiro, and P. B. Tavares, unpublished (2011).
[26]J. Agostinho Moreira, A. Almeida, W. S. Ferreira, J. E. Araújo, A. M. Pereira, M. R. Chaves, J. Kreisel, S. M. F. Vilela, and P. B. Tavares, Phys. Rev. B **81**, 054447 (2010).
[27]W. B. Holzapfel, Rep. Prog. Phys. **59**, 29 (1996).